Enzyme and Microbial Technology xxx (2008) xxx–xxx

Contents lists available at ScienceDirect

Enzyme and Microbial Technology

journal homepage: www.elsevier.com/locate/emt

# Inhibitors of *Bacillus anthracis* acetohydroxyacid synthase

Satish Kalme[a], Chien Ngoc Pham[a], Vinaykumar Gedi[a], Dung Tien Le[b], Jung-Do Choi[c], Sung-Kun Kim[d], Moon-Young Yoon[a,*]

[a] Department of Chemistry, Hanyang University, Seoul 133-791, Republic of Korea
[b] Department of Biochemistry, University of Nebraska-Lincoln, Lincoln, NE 68588, USA
[c] School of Life Sciences, Chungbuk National University, Cheongju 361-763, Republic of Korea
[d] Department of Chemistry and Biochemistry, Baylor University, Waco, TX 76798-7348, USA

ARTICLE INFO

*Article history:*
Received 31 December 2007
Received in revised form 26 February 2008
Accepted 27 February 2008

*Keywords:*
*Bacillus anthracis*
Acetohydroxy acid synthase
Herbicides
Uncompetitive inhibition
Docking

ABSTRACT

Twelve compounds (100 μM) had a predicted log *P* between −0.5 and −3.0 and inhibited AHAS activity by >40%. CE, IQ, and SMM showed dose-dependent inhibition of *Bacillus anthracis* AHAS (BAntx AHAS) with $IC_{50}$ values of 7.01 ± 0.81, 6.97 ± 0.44, and 10.02 ± 1.42 μM, respectively. CE and IQ were noncompetitive and uncompetitive inhibitors of BAntx AHAS with $K_{ii}$ values of 3.77 and 2.02, respectively. The order of potency towards BAntx AHAS was CE > PSE > MSM > TSM > SMM for sulfonylureas and IQ > Imazapic > IP for imidazolinones. The most active compound, CE, showed the lowest total interaction energy and highest MolDock score of −140.054 kcal/mol and −141.52, respectively. Three hydrogen bonds were identified between BAntx AHAS and CE. AHAS appears to be a promising potential target for new anti-anthracis drugs.



## 1. Introduction

Branched-chain amino acids (BCAAs) are synthesized by plants, algae, fungi, bacteria, and archaea, but not by animals. This makes the enzymes of the BCAA biosynthetic pathway potential targets for herbicides, fungicides, and antimicrobial compounds. The first common enzyme in the BCAA biosynthetic pathway is FAD- and thiamin-dependent acetohydroxyacid synthase (AHAS, EC 2.2.1.6) [1]. Sulfonylureas and imidazolinones, the most popular herbicidal AHAS inhibitors currently on the market for broad-spectrum weed control in major crops, are highly selective, potent, and nontoxic to animals [2,3]. Pyrimidinylthiobenzoates [4] and phthalazin-1(2H)-one derivative [5] also constitute an important kind of herbicides targeting acetohydroxyacid synthase. Xi et al. [6] have described a general quantum chemical descriptor for sulfonylurea analogues by characterizing the volume of electron cloud for specific substituent using the method of density functional theory. Until recently, amino acid biosynthesis has not been considered for antibacterial targeting because amino acids were assumed to be freely available to intracellular pathogens from their hosts. However, work on leucine and isoleucine–valine–leucine auxotrophs of *Mycobacterium tuberculosis*$^{H37Rv}$ [7], leucine auxotrophs of *Mycobacterium bovis* BCG [8], and an AHAS mutant of *Burkholderia pseudomallei* [9] has revealed that AHAS from pathogenic microorganisms shows potential as a target for antimicrobial agents.

Anthrax infection may result from exposure to spores of *Bacillus anthracis* by cutaneous, gastrointestinal, or aerosol routes, and may be characterized by extensive bacteremia and toxemia. With the emergence of *B. anthracis* spores as a possible weapon of terror, the development of new therapies is essential [10]. The utility of targeting the virulence factors of *B. anthracis* has been explored. To this end, protective antigen (PA) has been an attractive target, because this receptor-binding subunit allows entry of both the edema factor (EF) and lethal factor (LF) virulence factors into the cell/cytosol [11]. Several recent studies have shown that polyclonal antibodies against PA, as well as small-molecules and protein inhibitors of PA and/or LF, have therapeutic potential *in vitro* and in animal models [review in 11]. At present, however, several concerns have been raised about the vaccine, including lot-to-lot variation in the amount of PA in the vaccine [12] and occasional reactogenicity after vaccination [13].

These issues indicate a need to study alternative solutions, such as the possible application of herbicidal AHAS inhibitors as antimicrobial agents. A chemical bank of 26 herbicides was screened for *in vitro* inhibition of *B. anthracis* AHAS (BAntx AHAS). *In vivo* inhibition of AHAS enzyme activity by selected inhibitors and binding sites of the BAntx AHAS–CE complex was evaluated.

*Abbreviations:* BCAAs, branched-chain amino acids; BAntx AHAS, *Bacillus anthracis* AHAS; CE, chlorimuronethyl; IP, imazapyr; IQ, imazaquin; MSM, metsulfuronmethyl; NS, nicosulfuron; PSE, pyrazosulfuronethyl; PSM, primisulfuronmethyl; SMM, sulfometuronmethyl; TS, triasulfuron; TSM, thifensulfuronmethyl.

* Corresponding author. Tel.: +82 2 22200946; fax: +82 2 22990762.
*E-mail address:* myyoon@hanyang.ac.kr (M.-Y. Yoon).

0141-0229/$ – see front matter © 2008 Elsevier Inc. All rights reserved.
doi:10.1016/j.enzmictec.2008.02.011

## 2. Materials and methods

### 2.1. Expression and purification of AHAS

The plasmid pET28a, encoding the BAntx AHAS, was transformed into *Escherichia coli* BL21(DE3). Growth of the cells, induction of expression, and purification of overexpressed proteins were conducted according to previously described methods [14].

### 2.2. Microplate assay for AHAS

AHAS activity was assayed using the method of Singh et al. [15] with some modifications. In brief, each chemical in the library was dissolved in dimethyl sulfoxide (DMSO). The 200 μL reaction mixtures contained 50 mM $K_2HPO_4/KH_2PO_4$; pH 7.4, 1 mM ThDP, 10 mM $MgCl_2$, 50 μM FAD and 0.8 μg enzymes in individual wells of a 96-well microplate. Final pyruvate concentration was 75 mM. The acetoin formed was quantified at $A_{525}$ ($\varepsilon = 20{,}000\ M^{-1}\ cm^{-1}$) using a Spectra Max 340 spectrophotometer (Molecular Devices, Sunnyvale, USA). One unit (U) of activity was defined as the amount of enzyme required for the production of 1 μmol of acetolactate per minute under the assay conditions described above. All kinetic studies were performed using a discontinuous colorimetric assay with inhibitors of various concentrations as appropriate for the particular experiment.

### 2.3. log P prediction and preparation of the macromolecule

The ACD/log *P* program was used to calculate the log *P* (octanol/water partition coefficient) value of the bank of 26 herbicides. The ACD/log *P* algorithm is based on well-characterized log *P* contributions of separate atoms, structural fragments, and intramolecular interactions between different fragments [16]. In order to build a model for AHAS, the BAntx AHAS catalytic subunit amino acid sequence was first aligned with the *Arabidopsis thaliana* AHAS sequence using the program BioEdit [17]. The alignment was adjusted manually and the resulting sequences were fitted on to the X-ray coordinate structure of *A. thaliana* using the Deep View program. The resulting alignment was examined manually and submitted for automatic modeling at the Swiss-Homology Model server [18]. The initial model was improved by energy minimization. The force field used for energy minimization was a conjugate gradient (50 steps) provided by Deep View [19].

### 2.4. Molecular docking

MolDock (MVD), based on a new heuristic search algorithm that combines differential evolution with a cavity prediction algorithm, was used for docking studies [20]. The crystal structures of *A. thaliana* AHAS in complex with CE (pdb code 1N0H), IQ (pdb code 1Z8N), and SMM (pdb code 1YI0) were used as the basis of the docking experiments. We maintained only the particular ligand environment of *A. thaliana* AHAS structure to carry out molecular dockings. The hydrogens and bond orders were assigned to both ligand and protein molecules using automatic preparation function in MVD. For each complex, charges and protonation states were assigned using docking scoring function, and all acyclic single bonds were set as flexible, except for bonds that only rotated hydrogens. During the docking experiments, structural water molecules were excluded. Cofactors and metal ions were retained.

MolDock scoring function (grid resolution 0.30 Å) was used to precompute score grids for rapid dock evaluation. The ligand from the template was kept as a reference ligand. Potential binding sites (cavities) were detected using the grid-based cavity prediction algorithm. The population size, maximum iterations, scaling factor, and crossover rate were set to 50, 2000, 0.50, and 0.90, respectively. For each benchmark complex, we conducted ten independent runs with the MolDock optimizer algorithm, with each run returning one solution (pose). The highest ranked solution was compared with the known experimental structure using the standard Cartesian root-mean-square deviation (RMSD) measure (between similar atoms in the pose and experimental structure). Similar poses were clustered depending upon an RMSD threshold of 1.00 Å. The guided differential evolution and a force-field based docking scoring function were used to search the binding orientation and conformation of each candidate molecule. The saved pose for the ligand–enzyme complex of each molecule was subjected to detailed 3D analysis for interactions at the enzyme active site. Structural illustrations were created by Molegro Virtual Docker under the 'Windows XP' operating system installed on an Intel Pentium IV PC with a 2.8 MHz processor and 512 RAM.

### 2.5. In vivo inhibition of BAntx AHAS

CE was dissolved in DMSO and used at final concentration of 1–1.5 mM in 4 mL glucose–glutamate–glycine-salts (GGGS) synthetic medium [21]. One percent inoculum of *E. coli* BL21 (carrying BAntx AHAS gene), grown in Luria-Bertani medium for 10 h, was added in GGGS medium with or without CE and incubated at 120 rpm at 37 °C for 15 h. Growth of microorganism was determined at $A_{600}$. AHAS activity was determined in both the samples after 13 h of culture from cell-free extracts prepared as reported previously [14].

## 3. Results

### 3.1. Expression and purification of AHAS

SDS-PAGE analysis of transformed bacteria, before and after induction of the putative AHAS with IPTG (0.4 mM), showed increased intensity bands near to the expected size of the large (catalytic) subunit of BAntx AHAS. The purified protein was estimated to be 96% homogeneous by SDS-PAGE (data not shown).

### 3.2. log P analysis and screening of AHAS inhibitors

We calculated log *P* values of the compounds in the herbicide database with the ACD/log *P* program and picked out those compounds with a predicted log *P* between 0.5 and 3.0 (data not shown). *In vitro* inhibition of BAntx AHAS by 20 selected compounds was studied using a discontinuous colorimetric assay method.

Screening of the library identified 12 herbicides belonging to three groups of commercial herbicides (sulfonylureas, imidazolinones, and triazolopyrimidine) that inhibited BAntx AHAS activity ≥40% at a concentration of 100 μM. The sulfonylurea herbicides CE and SMM and the imidazolinone IQ were potent inhibitors of AHAS. The triazolopyrimidine herbicides TS, PSE, and NS weakly inhibited BAntx AHAS, and imazosulfuron, 1-[(3-fluro-2-propionyl-phenyl)-dihydroxy-methyl]-3-(4-methoxy-6-methyl-[1,3,5]triazin-2-yl)-urea, and 1-{dihydroxy-[4-(3,6,8-trioxa-bicyclo[3,2,1]oct-5-yl)-thiophen-3-yl]-methyl}-3-(4-methoxy-6-methyl-[1,3,5]triazin-2-yl)-urea exerted no inhibitory effect up to concentrations of 100 μM (data not shown). The 50% inhibition concentration ($IC_{50}$) (data not shown) for the 12 selected herbicides was analyzed by fit to

$$v = \frac{(V_0 - V_f)IC_{50}}{IC_{50} + [I]} + V_f \quad (1)$$

where $V_0$ is the reaction rate without inhibitor, $V_f$ is the rate at maximal inhibition, and $[I]$ is the inhibitor concentration. In a dose-dependent manner, inhibition of the catalytic subunit of BAntx AHAS by CE, IQ, and SMM corresponded to $IC_{50}$ values of 7.01 ± 0.81, 6.97 ± 0.44, and 10.02 ± 1.42 μM, respectively (Fig. 1).

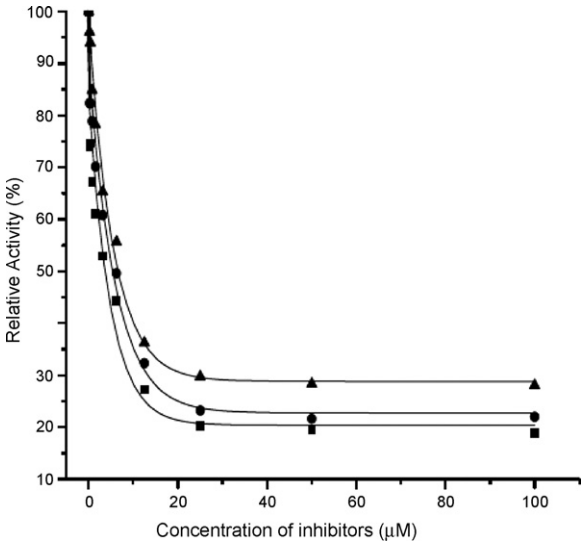


**Fig. 1.** Relative activity of BAntx AHAS as a function of the inhibitor concentration. (■) CE; (●) IQ; and (▲) SMM.

Please cite this article in press as: Kalme S, et al., Inhibitors of *Bacillus anthracis* acetohydroxyacid synthase, Enzyme Microb Technol (2008), doi:10.1016/j.enzmictec.2008.02.011

**Table 1**
BAntx AHAS inhibition kinetics and mechanisms of sulfonylurea (SU) and imidazolinones (IM)

| Class | Chemical | $K_{ii}$ (μM) | $K_{is}$ (μM) | Inhibition mechanism |
|---|---|---|---|---|
| SU | CE | 3.77 ± 0.86*** | 5.74 ± 1.34$$ | Noncompetitive |
| | SMM | 27.8 ± 3.44 | 5.05 ± 1.34$$ | |
| | MSM | 11.73 ± 2.20 | 26.36 ± 1.69 | |
| | PSE | 11.64 ± 3.31 | 11.06 ± 3.41$ | |
| IM | TSM | 22.25 ± 2.64 | 9.08 ± 2.90$ | Uncompetitive |
| | IQ | 2.02 ± 0.23*,*** | – | |
| | IP | 14.28 ± 1.28 | – | |
| | Imazapic | 9.13 ± 0.72 | – | |

Values are the mean of three experiments ± SEM. *Significantly different from IP at $P < 0.05$. ***Significantly different from SMM and TSM at $P < 0.001$. Significantly different from MSM at $P < 0.01 and $$P < 0.001 by one-way ANOVA with Tukey–Kramer multiple comparisons test.

### 3.3. Inhibition mechanism

Among these hit compounds, some herbicides were selected as representative structures to access their inhibition mechanism. The values of $K_{ii}$ and $K_{is}$ were determined by fitting Eq. (2) (noncompetitive inhibition) and (3) (uncompetitive inhibition) to the data (Table 1):

$$v = \frac{V_{max} \times [S]}{\{K_m(1 + [I]/K_{is} + [S](1 + [I]/K_{ii}\}} \quad (2)$$

$$v = \frac{V_{max} \times [S]}{\{K_m + [S](1 + [I]/K_{ii})\}} \quad (3)$$

In this equation, [S] and [I] are the concentrations of pyruvate and inhibitor, respectively. $K_{is}$ is a slope inhibition constant and $K_{ii}$ is an intercepts inhibition constant.

### 3.4. Homology modeling and docking analysis

The polypeptide of the catalytic subunit of BAntx AHAS has about 44% amino acid sequence identity and 60% sequence similarity to *A. thaliana* AHAS (data not shown) by needle method (default parameters), using EMBOSS pairwise alignment algorithms. We obtained the monomer of BAntx AHAS containing three domains, based on coordinates of *A. thaliana* AHAS (1YBH, 1Z8N and 1YI0), for individual selected herbicides (CE, IQ and SMM, respectively). The RMS *Z*-scores (close to 1.0) obtained by WhatCheck [22] imply that it is highly likely that the BAntx AHAS polypeptide is folded in the same general manner as *A. thaliana* AHAS (data not shown). The Ramachandran plot obtained during stereochemical analysis by PROCHECK [23] indicated that the overall conformation of the backbone of the model was reliable (Fig. 2). Glycine and proline were ignored and >99% of the residues located in the allowed regions. The docking of inhibitors of BAntx AHAS resulted in poses ≤1.00 Å RMSD threshold. After re-ranking, the poses showing maximum MolDock scores were selected (Table 2). The most active compound, CE, revealed lower total interaction energy and the highest MolDock score of −140.054 and −141.52 kcal/mol, respectively, indicating that CE had a higher binding affinity than IQ or SMM.

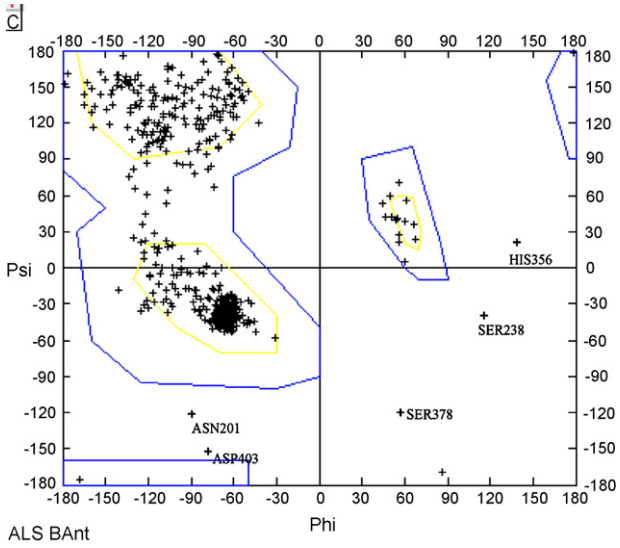


**Fig. 2.** Ramchandran plot of homology-modeled BAntx AHAS, derived by using Deep View/Swiss-PdbViewer 3.7. Labeled residues are in the disallowed regions.

### 3.5. Binding modes of the ligands

The aromatic ring of CE is rotated away from the axis of the sulfonylurea bridge and the aromatic ring substituent (such as the ethyl carboxy ester group) is positioned parallel with the atoms of the sulfonylurea bridge. This conformation of BAntx AHAS is similar to that observed in the case of the *A. thaliana*–CE complex [1]. There are three hydrogen bonds between BAntx AHAS and CE. The N atom of Gly46 is hydrogen bonded with the O atom of the sulfonylurea bridge (2.646 Å). The O atom of the methoxy substituent on the pyrimidine ring forms a hydrogen bond with the Ser92 O atom (3.286 Å). The $N_{14}$ atom of the pyrimidine ring contributes another hydrogen bond with the Gln131 O atom (2.557 Å) (Fig. 3). These interactions establish the stable binding mode and orientation of the BAntx AHAS–CE complex. The other BAntx AHAS amino acids likely to be involved in hydrophobic and van der Waals interactions are Gly45, Ala47, Leu49, Phe130, and Lys180. Some of these residues are equivalent in *A. thaliana*; Phe130 is Phe206, Gln131 is Gln207, and Lys180 is Lys256 [1]. Despite major similarities between CE and SMM, the absence of the methoxy substituent on the pyrimidine ring results in a low binding affinity for SMM (Table 2).

### 3.6. In vivo inhibition of BAntx AHAS

Inhibition of *E. coli* BL21 (BAntx AHAS) growth in the presence of CE was studied at two different concentrations (Fig. 4). A CE concentration of 1.5 mM inhibited 80% of growth in GGGS medium, giving a stationary phase of 6 h. A decrease in AHAS activity was recorded as the concentration of CE increased. Cells grown in the presence of 1.5 mM CE for 12 h showed ≥91% inhibition of

**Table 2**
The binding affinity and interaction energy between inhibitors and BAntx AHAS

| Compound | Binding affinity (kcal/mol) | Interaction[a] | Internal[b] | MolDock Score[c] |
|---|---|---|---|---|
| CE | −28.21 | −140.054 | −1.466 | −141.52 |
| IQ | −20.59 | −130.906 | −1.233 | −132.13 |
| SMM | −21.68 | −128.201 | −1.822 | −130.02 |

[a] Interaction: total interaction energy (ligand + BAntx AHAS).
[b] Internal: the internal energy of the ligand.
[c] Docking scoring function by MolDock.

Please cite this article in press as: Kalme S, et al., Inhibitors of *Bacillus anthracis* acetohydroxyacid synthase, Enzyme Microb Technol (2008), doi:10.1016/j.enzmictec.2008.02.011

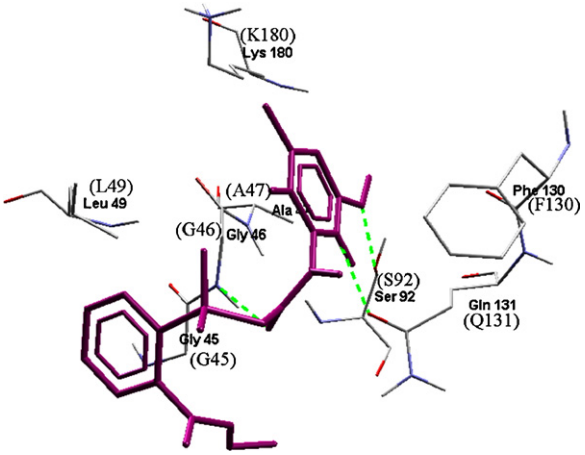


**Fig. 3.** Binding mode of CE to BAntx AHAS. Green lines indicate the hydrogen bonds. (For interpretation of the references to color in this figure legend, the reader is referred to the web version of the article.)

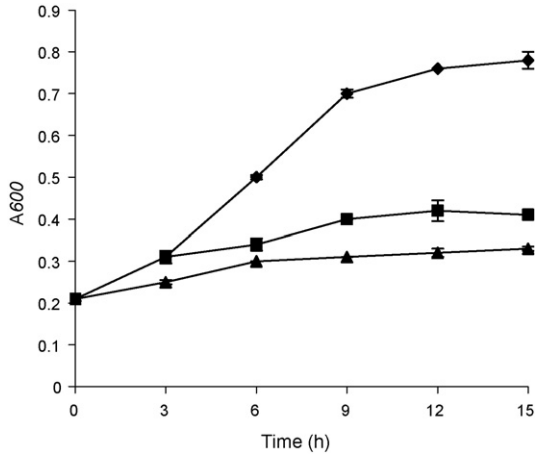


**Fig. 4.** Time course of *Escherichia coli* BL21 (BAntx AHAS) growth in the presence or absence of CE in GGGS medium. (♦) Without CE (1% DMSO, v/v); (■) 1 mM CE; and (▲) 1.5 mM CE.

AHAS activity compared to control cells (*E. coli* BL21 containing BAntx AHAS) grown without inhibitor (data not shown). *In vivo* AHAS inhibition by CE was in general accordance with its *in vitro* activity.

## 4. Discussion

We sought to identify new templates for possible anti-anthracis drugs that would inhibit AHAS, which catalyzes the first common step in the biosynthetic pathway of the branched amino acids. This study is the first to describe the inhibition kinetics of BAntx AHAS, which was expressed in *E. coli* and purified to homogeneity. The biochemical characteristics and substrate and cofactor requirements of recombinant BAntx AHAS have previously been described [14]. The specific activity of the catalytic subunit (1.5 U/mg) was not inferior to AHAS from *M. tuberculosis* (2.8 U/mg) [24] or *M. avium* (3.8 U/mg) [25]. We have not used small (regulatory) subunit to make holoenzyme, as catalytic subunit alone has been reported to show AHAS activity [24].

Hydrophobicity is an important factor that can determine whether a given pharmaceutical compound can effectively reach its site of action. In this study, the solubility nature (based on log *P* analysis) was better for SMM compared to any other herbicides and all values produced were between −0.7 and 3.33. This finding is in agreement with Lipinski et al. [26] that most commercial herbicides have a log *P* value between −0.5 and 3.0. Of the twelve herbicides studied, only CE, SMM, and IQ strongly inhibited BAntx AHAS. The $IC_{50}$ values of CE and SMM were similar in magnitude to those reported for *M. tuberculosis* [24] and *M. avium* [25]. Interestingly, IQ and other herbicides from the imidazolinones group (Fig. 5) showed promising inhibition of BAntx AHAS, but no or very poor inhibition for most of the AHASs reported (Table 3). The other herbicides, except PSM (Fig. 5), were moderately good inhibitors of BAntx AHAS, with the lowest $IC_{50}$ values ranging from 15 to 23 mM (Table 3).

The sulfonylureas have been reported to be mixed [27], uncompetitive [28], and nearly competitive inhibitors with respect to pyruvate [29]. IQ ($K_{ii}$ 2.02 μM) was an uncompetitive inhibitor for the catalytic subunit of BAntx AHAS. The $K_{ii}$ value of 9.13 μM of Imazapic was not significantly inferior to that of IQ. Structural analysis of these herbicides revealed that a substitution by benzene at R1 significantly increases the inhibition of BAntx AHAS. In the case of IP, where no substitution was allowed at R1 and R2, we observed a seven-fold increase in the $K_{ii}$ value compared to IQ. The benzene ring, which participates in major interactions in ligand binding, is absent in both IP and Imazapic. These extra contacts may help to explain the observed order of potency towards BAntx AHAS of IQ > Imazapic > IP. In *A. thaliana* AHAS, the order of potency was IQ > Imazethapyr > IP [30]. Considering the substitution pattern and $K_{ii}$ values of the sulfonylureas studied, the replacement of a formic acid methyl ester with a formic acid ethyl

**Table 3**
Inhibition of AHAS from BAntx and other organisms by different herbicides

| AHAS | Sulfonylureas[a] | | | | | | Imidazolinones[a] | | |
|---|---|---|---|---|---|---|---|---|---|
| | CE | SMM | NS | PSM | TS | MSM | IQ | IP | Imazapic |
| *Bacillus anthracis*[b] | 7.01 ± 0.81 | 10.02 ± 1.42 | 15.88 ± 2.81 | 12.85 ± 8.76 | 16.07 ± 4.63 | 21.91 ± 8.99 | 6.97 ± 0.44 | 21.81 ± 5.61 | 23.47 ± 6.77 |
| *Mycobacterium tuberculosis*[c] | 8.97 | 4.79 | WI[d] | 4.19 | WI[d] | 5.96 | NI | NI | NI |
| *M. avium*[e] | ND | 13.5 ± 0.6 | ND | 18.3 ± 1 | 39.6 ± 3.6 | 39 ± 1.6 | >1000 | >2000 | ND |
| *Escherichia coli* isozyme II[f] | ND | 0.8 ± 0.06 | ND | 0.5 ± 0.03 | 0.17 ± 0.001 | 0.056 ± 0.007 | 110 ± 10 | >1000 | ND |
| *E. coli* isozyme III[g] | ND | 190 ± 30 | ND | 184 ± 17 | 56 ± 2 | 55 ± 3 | >1000 | >500 | >500 |
| *Bacillus stearothermophilus*[h] | ND | 11.7 | ND | ND | ND | ND | ND | ND | ND |

WI: weak inhibition, NI: no inhibition, ND: not determined.
[a] $IC_{50}$ for inhibitor (μM).
[b] From this study.
[c] Data taken from [26].
[d] Inhibited to < 70% at 40 μM.
[e] Data taken from [27].
[f] Data taken from [34].
[g] Data taken from [35].
[h] Data taken from [36].

Please cite this article in press as: Kalme S, et al., Inhibitors of *Bacillus anthracis* acetohydroxyacid synthase, Enzyme Microb Technol (2008), doi:10.1016/j.enzmictec.2008.02.011

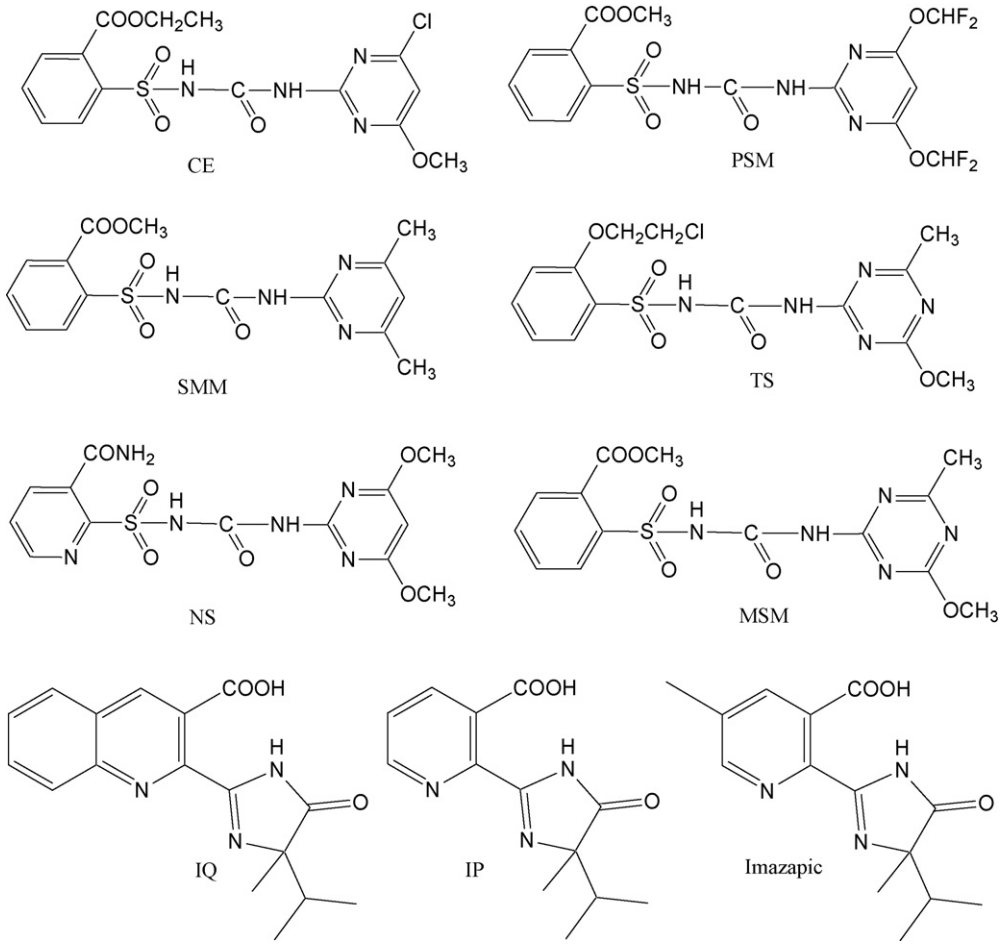


**Fig. 5.** Structures of sulfonylureas and Imidazolinones used in this study. Inhibition of AHAS from BAntx and other organisms by these herbicides is compared in Table 3.

ester at the R1 position reduced the $K_{ii}$ value by 1.5–9-fold. This finding implies that when larger substituents are present on the aromatic ring, maximum interactions can develop between the aromatic ring of sulfonylurea and amino acids in the tunnel leading to the active site. In *S. cerevisiae* [31,32] and *A. thaliana* [33] AHAS, the terminal methyl group of the carboxy ester substituent and methoxy substituent on the heterocyclic ring (CE) have significant roles in hydrophobic interactions with the dimethylbenzene ring of FAD and other amino acids. We observed CE ($K_{ii}$ 3.77 μM) to be a potent inhibitor, with a potency order of CE > PSE > MSM > TSM > SMM.

In conclusion, the BAntx AHAS shares some equivalent residues with other AHAS macromolecules, but some unique residues interact with CE. These new binding sites are of interest in the design of novel inhibitors of BAntx AHAS. The results presented here imply that the inhibition of AHAS by CE and IQ is a direct measure of the interaction between the enzyme and the inhibitor. Further screening of analogues of CE and IQ, and improved understanding of their interaction with BAntx AHAS will be instrumental in developing better BAntx AHAS inhibitors, and a new approach to controlling anthracis.

## Acknowledgment

This work was supported by the research fund of Hanyang University (HY2006-I).

## References

[1] McCourt JA, Duggleby RG. Acetohydroxyacid synthase and its role in the biosynthetic pathway for branched-chain amino acids. Amino Acids 2006;31:173–210.
[2] Shaner DL, Singh BK. Acetohydroxyacid synthase inhibitors. In: Roe M, Burton JD, Kuhr RJ, editors. Herbicide activity: toxicology, biochemistry and molecular biology. Amsterdam: IOS Press; 1997. p. 69–110.
[3] Yang G, Liu H, Yang H. QSAR and 3D-QSAR analysis of structurally diverse ALS inhibitors: sulfonylureas and triazolopyrimidine-2-sulfonamides. Pestic Sci 1999;55:1143–50.
[4] He Y-Z, Li Y-X, Zhu X-L, Xi Z, Niu C, Wan J, et al. Rational design based on bioactive conformation analysis of pyrimidinylbenzoates as acetohydroxyacid synthase inhibitors by integrating molecular docking, CoMFA, CoMSIA, and DFT calculations. J Chem Inf Model 2007;47:2335–44.
[5] Li Y-X, Luo Y-P, Xi Z, Niu C, He Y-Z, Yang G-F. Design and syntheses of novel phthalazin-1(2H)-one derivatives as acetohydroxyacid synthase inhibitors. J Agric Food Chem 2006;54:9135–9.
[6] Xi Z, Yu Z, Niu C, Ban S, Yang G. Development of a general quantum-chemical descriptor for steric effects: density functional theory based QSAR study of herbicidal sulfonylurea analogues. J Comput Chem 2006;27:1571–6.
[7] Guleria I, Teitelbaum R, McAdam RA, Kalpana G, Jacobs Jr WR, Bloom BR. Auxotrophic vaccines for tuberculosis. Nat Med 1996;2:334–7.
[8] Bange FC, Brown AM, Jacobs Jr WR. Leucine auxotrophy restricts growth of *Mycobacterium bovis* BCG in macrophages. Infect Immun 1996;64:1794–9.
[9] Atkins T, Prior RG, Mack K, Russell P, Nelson M, Oyston PC, et al. A mutant of *Burkholderia pseudomallei*, auxotrophic in the branched chain amino acid biosynthetic pathway, is attenuated and protective in a murine model of melioidosis. Infect Immun 2002;70:5290–4.
[10] David LB, Douglas KO, Paul S, John F, Mark AM. Detection of an inhalational anthrax outbreak. Emerg Infect Dis 2006;12:1942–9.
[11] Huber M, Vor Dem Esche U, Grunow R, Bessler WG. Generation of mouse polyclonal and human monoclonal antibodies against *Bacillus anthracis* toxin. Drugs Exp Clin Res 2005;31:35–43.
[12] Committee to assess the safety and efficacy of the anthrax vaccine MFA. In: Joellenbeck LM, Zwanziger LL, Durch JS, Strom BL, editors. The anthrax vac-

Please cite this article in press as: Kalme S, et al., Inhibitors of *Bacillus anthracis* acetohydroxyacid synthase, Enzyme Microb Technol (2008), doi:10.1016/j.enzmictec.2008.02.011

cine: is it safe? Does it work? Washington, DC: National Academies Press; 2002.
[13] Wasserman GM, Grabenstein JD, Pittman PR, Rubertone MV, Gibbs PP, Wang LZ. Analysis of adverse events after anthrax immunization in US Army medical personnel. J Occup Environ Med 2003;45:222–33.
[14] Choi KJ, Pham CN, Jung H, Han SH, Choi JD, Kim J, et al. Expression of acetohydroxyacid synthase from *Bacillus anthracis* and its potent inhibitors. Bull Korean Chem Soc 2007;28:1109–13.
[15] Singh BK, Stidham MA, Shaner DL. Assay of acetohydroxyacid synthase. Anal Biochem 1988;171:173–9.
[16] Williams A, Kolovanov E. A rebuttal regarding recent comparisons of SciLogP ultra (Scivision Inc.) with ACD/log *P* prediction software. In: Procedings of the log *P* 2000 symposium. 2000. p. 1–23.
[17] Hall TA. BioEdit: a user-friendly biological sequence alignment editor and analysis program for Windows 95/98/NT. Nucleic Acids Symp Ser 1999;41:95–8.
[18] Schwede T, Kopp J, Guex N, Peitsch MC. SWISS-MODEL: an automated protein homology-modeling server. Nucleic Acids Res 2003;31:3381–5.
[19] Guex N, Peitsch MC. Swiss-model and the Swiss-PdbViewer: an environment for comparative protein modeling. Electrophoresis 1997;18:2714–23.
[20] Thomsen R, Christensen MH, MolDock:. A new technique for high-accuracy molecular docking. J Med Chem 2006;49:3315–21.
[21] Buono F, Testa R, Lundgren DG. Physiology of growth and sporulation in *Bacillus cereus*. I. Effect of glutamic and other amino acids. J Bacteriol 1966;91:2291–9.
[22] Vriend GJ. WHAT IF: a molecular modeling and drug design program. Mol Graph 1990;8:52–6.
[23] Laskowski RA, MacArthur MW, Moss DS, Thornton JM. PROCHECK: a program to check the stereochemical quality of protein structures. J Appl Cryst 1993;26:283–91.
[24] Choi KJ, Yu YG, Hahn HG, Choi JD, Yoon MY. Characterization of acetohydroxyacid synthase from *Mycobacterium tuberculosis* and the identification of its new inhibitor from the screening of a chemical library. FEBS Lett 2005;579:4903–10.
[25] Zohar Y, Einav M, Chipman DM, Barak Z. Acetohydroxyacid synthase from *Mycobacterium avium* and its inhibition by sulfonylureas and imidazolinones. Biochim Biophys Acta 2003;1649:97–105.
[26] Lipinski CA, Lombardo F, Dominy BW, Feeney P. Experimental and computational approaches to estimate solubility and permeability in drug discovery and development settings. J Adv Drug Deliv Rev 1997;23:3–25.
[27] Hill CM, Pang SS, Duggleby RG. Purification of *Escherichia coli* acetohydroxyacid synthase isoenzyme II and reconstitution of active enzyme from its individual pure subunits. Biochem J 1997;327:891–8.
[28] Xing RY, Whitman WB. Sulfometuron methyl-sensitive and -resistant acetolactate synthases of the achaebacteria *Methanococcus* spp. J Bacteriol 1987;169:4486–92.
[29] Ahan TW, Kim DW, Choi JD. Inhibition of acetohydroxyacid synthase by sulfonylureas and imidazolinones. Korean Biochem J 1992;25:636–41.
[30] Chang AK, Duggleby RG. Herbicide-resistant forms of *Arabidopsis thaliana* acetohydroxyacid synthase: characterization of the catalytic properties and sensitivity to inhibitors of four defined mutants. Biochem J 1998;333:765–77.
[31] Pang SS, Guddat LW, Duggleby RG. Molecular basis of sulfonylurea herbicide inhibition of acetohydroxyacid synthase. J Biol Chem 2003;278:7639–44.
[32] McCourt JA, Pang SS, Duggleby RG, Guddat LW. Elucidating the specificity of binding of sulfonylurea herbicides to acetohydroxyacid synthase. Biochemistry 2005;44:2330–8.
[33] McCourt JA, Pang SS, King-Scott J, Duggleby RG, Guddat LW. Herbicide binding sites revealed in the structure of plant acetohydroxyacid synthase. Proc Natl Acad Sci USA 2006;103:569–73.
[34] Bar-Ilan A, Balan V, Tittmann K, Golbik R, Vyazmensky M, Hu¨bner G, et al. Binding and activation of thiamin diphosphate in acetohydroxyacid synthase. Biochemistry 2001;40:11946–54.
[35] Vyazmensky M, Sella C, Barak Z, Chipman DM. Isolation and characterization of subunits of acetohydroxy acid synthase isozyme III and reconstitution of the holoenzyme. Biochemistry 1996;35:10339–46.
[36] Porat I, Vinogradov M, Vyazmensky M, Lu CD, Chipman DM, Abdelal AT, et al. Cloning and characterization of acetohydroxyacid synthase from *Bacillus stearothermophilus*. J Bacteriol 2004;186:570–4.

Please cite this article in press as: Kalme S, et al., Inhibitors of *Bacillus anthracis* acetohydroxyacid synthase, Enzyme Microb Technol (2008), doi:10.1016/j.enzmictec.2008.02.011